Studies with Improved Renormalization Group Techniques

by

Gregory James Petropoulos

B.S., University of Connecticut, 2010

M.S., University of Colorado, 2013

A thesis submitted to the

Faculty of the Graduate School of the

University of Colorado in partial fulfillment

of the requirements for the degree of

Doctor of Philosophy

Department of Physics

2015

This thesis entitled:
Studies with Improved Renormalization Group Techniques
written by Gregory James Petropoulos
has been approved for the Department of Physics

Anna Hasenfratz

Prof. Thomas DeGrand

Prof. Ethan Neil

Prof. Senarath de Alwis

Prof. Thomas A. Manteuffel

Date _____

The final copy of this thesis has been examined by the signatories, and we find that both the content and the form meet acceptable presentation standards of scholarly work in the above mentioned discipline.

Petropoulos, Gregory James (Ph.D., Physics)

Studies with Improved Renormalization Group Techniques

Thesis directed by Prof. Anna Hasenfratz

Dedication

Acknowledgements

This thisis was supported by an award from the Department of Energy (DOE) Office of Science Graduate Fellowship Program (DOE SCGF). The DOE SCGF Program was made possible in part by the American Recovery and Reinvestment Act of 2009. The DOE SCGF program is administered by the Oak Ridge Institute for Science and Education for the DOE. ORISE is managed by Oak Ridge Associated Universities (ORAU) under DOE contract number DE- AC05-06OR23100. All opinions expressed in this presentation are the author's and do not necessarily reflect the policies and views of DOE, ORAU, or ORISE.

Contents

Tables

Table

Figures

Figure

Chapter 1

Monte Carlo Renormalization Group

1.1 Introduction

In recent years, many groups have initiated lattice investigations of strongly-coupled gauge–fermion systems beyond QCD. While the ultimate goal of these efforts is to explore potential new physics beyond the standard model, an essential step is to improve our theoretical understanding of the basic properties of these non-perturbative systems. In this chapter I study the renormalization group properties of SU(3) gauge theories with $N_f = 8$ and 12 nearly-massless fermions in the fundamental representation, through the Monte Carlo Renormalization Group (MCRG) two-lattice matching technique. This is one of several complementary analyses our group is involved with, two more of which (investigating Dirac eigenmode scaling and finite-temperature transitions) are discussed elsewhere [67, 107]. Recent references on SU(3) gauge theories with $N_f = 8$ and 12 include [48, 49, 6, 40, 86]; earlier works are reviewed in Ref. [56].

References [66, 65] study MCRG two-lattice matching for the 12-flavor system with nHYP-smeared staggered actions very similar to those we use here. Our gauge action includes both fundamental and adjoint plaquette terms, with coefficients related by $\beta_A = -0.25\beta_F$. The negative adjoint plaquette term lets us avoid a well-known spurious ultraviolet fixed point caused by lattice artifacts, and implies $\beta_F = 12/g^2$ at the perturbative level. In our fermion action, we use nHYP smearing with parameters $(0.5, 0.5, 0.4)$, instead of the $(0.75, 0.6, 0.3)$ used by Refs. [66, 65]. By changing the nHYP-smearing parameters in this way, we can access stronger couplings without encountering numerical problems. At such strong couplings, for both $N_f = 8$ and $N_f = 12$ we

observe a lattice phase in which the single-site shift symmetry ("S^4") of the staggered action is spontaneously broken ("$\not{S}^4$") [28, 107].[1] In this work we only investigate couplings weak enough to avoid the $\not{S}^4$ lattice phase.

In the next section, we review how the MCRG two-lattice matching technique determines the step-scaling function s_b in the bare parameter space. Although working entirely with bare parameters would be disadvantageous if our aim were to produce renormalized phenomenological predictions for comparison with experiment, our current explorations of the phase structures of the 8- and 12-flavor systems benefit from this fully non-perturbative RG approach, especially for relatively strong couplings. In Section 1.3 we present our results from the traditional MCRG two-lattice matching technique. While our 8-flavor s_b is significantly different from zero, for $N_f = 12$ we observe $s_b \lesssim 0$ for $\beta_F < 8$, indicating an infrared fixed point (IRFP).

We emphasize that while the existence of an IRFP is physical (scheme-independent), the coupling at which it is located depends on the choice of renormalization scheme. A limitation of traditional MCRG two-lattice matching is the need to optimize the RG blocking transformation separately for each lattice coupling β_F. As we explain below, this optimization forces us to probe a different renormalization scheme for each β_F, so that the bare step-scaling function we obtain is a composite of many different discrete β functions. Chapter **??** discusses an improvement to traditional MCRG that avoids this issue.

1.2 Method

In this section I will discuss the basic procedure for MCRG. MCRG is a real space renormalization group technique that can be used to study the critical properties of statistical systems. The idea was first proposed by Kadanoff. However it wasn't until Wilson's work that it became a well defined quantitative technique. The process of MCRG can be broken into two primary steps:

(1) Blocking

[1] Ref. [40] recently interpreted the $\not{S}^4$ lattice phase in terms of relevant next-to-nearest neighbor interactions.

(2) Matching

Blocking integrates out the UV fluctuations, exposing the IR dynamics. Matching allows us to match pairs of couplings in such a way that we can measure the bare step scaling function. The steps scaling function is the discrete analog of the beta function in the continuum. In general it is possible to recover the beta function from the step scaling function. However, for our purposes this is not important. Our goal is to determine whether or not a particular theory is conformal in the IR. As long as strong enough couplings are studied, the IRFP will be visible in both the bare step scaling function and the renormalized beta function.

In the Wilsonian picture, couplings are characterized by their engineering dimension. In a four dimensional theory, a coupling is relevant if its engineering dimension is less than four. The coupling is marginal if its engineering dimension is equal to four and irrelevant if the engineering dimension is greater than four. The RG flow of the system is governed by fixed points and the renormalized trajectory. The sytems we study have a repulsive UV fixed point. If the theory is conformal it will also have an attractive IR fixed point. The renormalized trajectory originates at the UV fixed point and flows in relevant directions towards the infrared. Flow in irrelevant directions will always be directed towards the renormalized trajectory. Finally flow along the renormalized trajectory will always flow into attractive fixed points. In theories with multiple fixed points, the renormalized trajectory connects the fixed points in coupling space. Flow from an arbitrary point in coupling space will always be towards the renormalized trajectory in irrelevant or marginal directions and along the renormalized trajectory in relevant directions. Generally the flow should be fastest in irrelevant directions.

1.2.1 Blocking

The first step in MCRG is to block the lattice. Blocking requires that the theory is defined on a regular lattice that has a discrete scaling symmetry. Discrete scaling symmetry, shown in figure 1.1 simply means that you can divide the sites of the lattice into regular blocks that tile the entire lattice and then replace those blocks with a single site. The new site can be located at a site from

the original lattice or anywhere in the block. The value at this site is typically computed as some function of the sites in the blocking group. The lattice has a discrete scaling symmetry if [18]

(1) we perform this block replacement the same way to every block in the original lattice

(2) we scale the lattice spacing of the lattice formed by the block variables: $a \to a' \equiv sa$

(3) the lattice of block replaced observables is the same size as the original lattice

Here s is a scale factor which relates the original lattice to the blocked lattice.

The blocked lattice will have fewer sites than the original lattice. If the block variable has P sites from the original lattice and d dimensions then the relationship between the number of sites lost, the scale factor and the lattice dimension is $p = s^d$. Naturally the blocking process can be repeated in a recursive manner until blocking is no longer possible. As an example consider a 32^2 square lattice that is being blocked by a factor $s = 2$. Such a lattice can be blocked 4 times: $32^2 \to 16^2 \to 8^2 \to 4^2 \to 2^2$. Performing another blocking would result in a single point which doesn't have the same dimensionality as our initial $2 - D$ lattice. It is clear that some starting volumes are more flexible than others. A 14^2 lattice can only be blocked once, $14^2 \to 7^2$, since a 7^2 lattice can not be blocked with a scale factor of 2.

In a lattice simulation the quantities we are interested in are the link variables. The link variable $U_{n,\mu}$ encodes the gauge field at site n in all four $\hat{\mu}$ directions. A MCRG blocking step can be defined as a transformation that takes two links $U_{n,\mu}$ and $U_{n+\hat{\mu},\mu}$ and creates one link with twice the lattice spacing of the initial two links.

Employing a square blocking scheme as described above means the blocked lattice will have a factor of 2^N fewer links than the original lattice. In four dimensions this means that an observable such as a Wilson loop will have a factor of 16 less statistics on the blocked lattice compared to the original lattice. Fortunately, on an N dimensional hyper cubic lattice there are 2^N unique ways to perform this blocking. Therefore in four dimensions there are 16 unique blocking configurations. We can preserve statistics in our calculation by performing all of the unique blocking transformations and averaging all of the observables from those blocking transformations together. Additionally we

store the blocked links on a lattice of the original cardinality using offsets as shown in figure 1.2. This allows us to efficiently store a lattice blocked down to any allowable level and has the added benefit that only minor adjustments need to be made to our code to calculate blocked observables.

Lets consider how blocking will effect a lattice model with d dimensions and action $S(K_i)$. Here K_i are the set of all possible couplings in the action. In lattice simulations only a small number of these couplings are actually tuned. The system is characterized by one or more length scales i.e. the correlation length ξ. After blocking, the links have a lattice spacing scaled by s, $a' = sa$ such that the physical size of the box has not been changed. This removes the UV fluctuations below the length scale sa. Because the UV modes have been integrated out the blocked lattice is described by a new action S' with a new set of couplings $K_i^{n_b}$ where n_b is the number of blocking steps. As long as s is smaller than the lattice correlation length the infrared properties of the system are unaffected. Successive blocking steps will define a flow in coupling space:

$$K_i^{(0)} \to K_i^{(1)} \to K_i^{(2)} \to ... \to K_i^{(n_b)}, \tag{1.1}$$

where K_i^0 denotes the couplings on the unblocked lattice.

Although the physical correlation length is unchanged the lattice correlation length after n_b blocking steps is scaled by

$$\xi^{n_b} = s^{-n_b}\xi^{(0)}. \tag{1.2}$$

Critical fixed points exist when $\xi = \infty$ and trivial fixed points exist when $\xi = 0$. The scaling behavior at critical fixed points are well understood theoretically. Here the linearized RG transformation predicts the scaling operators and the corresponding scaling dimension.

Figure 1.3 visualizes the renormalization group flow that I have described for a system with one fixed point and only one relevant coupling at the fixed point, K_0. All other couplings are irrelevant and are collapsed onto the y-axis. The critical surface is shown in the figure is depicted at at $K_0 = 0$. A simulation point in parameter space, P, is chosen. The flow lines approach the fixed point in the irrelevant directions and flow away from the fixed point in the relevant direction. After some number of RG steps the irrelevant operators have died out and the system is flowing

along the renormalized trajectory. The renormalized trajectory is uniquely determined by the RG transformation.

Finally, in our blocking step we also apply a nHYP smearing step. By changing the parameters in the smearing step we can control the renormalized trajectory that we will flow to under successive blocking steps. If we start with an infinite volume the choice of nHYP parameters would be of little consequence because we could block our system an infinite number of times until we reach the renormalized trajectory. Unfortunately in the real world we are not afforded that luxury. It is necessary to choose a smearing that guarantees you can reach the renormalized trajectory in a finite number of steps. We accomplish this by applying a nHYP smearing to the unblocked lattice. We choose the three parameters of the nHYP smearing to be (α, 0.2, 0.2) where we use several values of α, $0.3 \leq \alpha \leq 0.7$. After smearing the unblocked lattice, we multiply adjacent links to form a single blocked link.

1.2.2 Two-lattice matching procedures and the need for optimization

The goal of two lattice matching is to determine a series of lattice couplings, $\beta_0, \beta_1, ...\beta_n, ...$, with lattice spacings that differ by a factor of s between consecutive points. That is $a(\beta_n) = a(\beta_{n-1})/s$. The scale change s is the same scale change as in the blocking discussion above. I denote the bare step scaling function as

$$s_b(\beta_n, s) = \beta_n - \beta_{n-1}. \tag{1.3}$$

The renormalized running coupling of theories governed by a Gaussian fixed point can be recovered with a bit of extra work. In weak coupling near the fixed point a renormalized coupling can be calculated. This coupling can be compared to a continuum regularization scheme. At stronger coupling a physical quantity or other quantity such as the Sommer parameter or the Wilson Flow is used to determine the lattice scale. Since the primary focus of this thesis is to determine the existence or lack thereof of an infrared fixed point in strong coupling I don't attempt to follow such a procedure. In the future finding the corresponding renormalized beta function may

be of interest.

Figure 1.4 demonstrates how two lattice matching is performed. In the figure we start with two points in coupling space P_1 and P_2. Under successive RG transformations they flow along the lines indicated. If we can identify two sets of couplings that flow to the same point on the renormalized trajectory after the same number of blocking steps we know that the correlation lengths are identical. From equation 1.2 we know that if two sets of couplings flow to the same point on the renormalized trajectory, but one set of couplings required one less blocking step that the lattice correlation length differers from a factor of s. Thus we have accomplished our goal. We have identified two points in coupling space P_1 and P_2 with corresponding $\xi_2 = \xi_1/s$ after n and $(n-1)$ blocking steps.

Demonstrating that the couplings are equal is equivalent to showing that the actions are identical, $S(P_1^{(n_b)}) = S(P_2^{(n_{b-1})})$. Calculating the blocked action is extremely challenging. Fortunately we don't have to do this. We are saved because we don't need to know the exact form of the actions to demonstrate that they are equivalent. Instead we can show that expectation values of every operator measured on $P_1^{(n_b)}$ and $P_2^{(n_b-1)}$ are identical. Generating configuration ensembles of blocked lattices with the approximate Boltzman weights is trivial, we simply need to take an existing ensemble of configurations and then block them [113].

Putting everything together we can prescribe the following procedure for two lattice matching [63]:

(1) Generate a configuration ensemble of size L^d with action $S(P_1)$. Block each configuration n_b times and measure a set of expectation values on the resulting $(L/s^{n_b})^d$ set.

(2) Generate several configurations of size $(L/s)^d$ with action $S(P_2)$, where each P_2 is a set of trial couplings. Block each configuration $(n_b - 1)$ times and measure the same expectation values on the resulting $(L/s^{n_b})^d$ set. Compare the results with that obtained in step 1 and tune the coupling P_2 such that the expectation values agree. If they do we have determined a flow $P_1 \to P_2$ over scale s.

This method is powerful for several reasons. Since we compare measurements on the same lattice size, the finite volume corrections are small. Working on lattices larger than the correlation length of the system is not required. MCRG works in both the confined and deconfined phases. Since the matching is accomplished from measurements of local operators, their computation is cheap and the statistical errors are small. Finally because the flow lines are unique it is sufficient to match only one operator. The other operators should give the same prediction. If we fail to reach the renormalized trajectory it will be evident in that the other operators do not match. Therefore we can use the spread in the matching values of the different operators as a measure of systematic error in our matching.

The discussion so far has focused on fixed points with one relevant operator. If the fixed point has two relevant operators the matching process is identical, only now it is necessary to tune two operators to find pairs of points in a two dimensional coupling space. While this is possible, it is much easier to fix one of the relevant couplings to its fixed point value. By effectively removing one of the relevant couplings we can proceed as with the matching of the remaining coupling.

There is one final hurdle to overcome. On a finite volume we only have a finite number of blocking steps. If we are unlucky we might choose a block transformation, and therefore a renormalized trajectory, that is so far away from the bare parameters in couplings space that we never approach it. Accordingly after we have performed the maximum number of blocking steps the system may not reach the renormalized trajectory. This is a problem because matching requires both blocked ensembles to have reached the renormalized trajectory.

One solution is to use a bigger volume. Using a bigger volume means that we can perform more blocking steps, eventually we will arrive at the renormalized trajectory. This solution is clearly flawed. Lets assume that the largest volume you have is 32^4 and you can not reach the renormalized trajectory in four blocking steps. To achieve one more blocking step you need to jump to 64^4 lattices, if that is not enough then on to 128^4 lattices. We are now considering lattices that are larger than those used for large professional calculations! The computational cost of configuration generation scales roughly as $V^{5/4}$, in our doubling scenario generating larger volumes

will require at least $2^{5/4}$ more computational power.

Clearly we need another solution. As I mentioned above we apply an nHYP smearing step during our block transformation. This serves a crucial role, nHYP smearing has 3 parameters. Since the different block transformations correspond to different renormalized trajectories, tuning the nHYP parameters allows us to control the renormalized trajectory that we flow to. We use the first parameter of the nHYP smearing as an optimization parameter and fix the second and third. We identify the optimal blocking accordingly:

(1) Consistent matching between the different operators: along the RT all expectation values should agree on the matched configuration sets. Any deviation is a measure that the RT has not been reached.

(2) Consecutive blocking steps should give the same matching coupling.

1.2.3 Chirally Broken Theories

In a confining and chiral broken theory, such as QCD, the RG flow will away from the repulsive UV fixed point into the IR. If the fermions are massless the only relevant operator is the gauge coupling β. This is the β that we set in the action of our lattice simulation. Therefore the renormalized trajectory will flow along the β axis in coupling space from infinity to zero. RG flows will flow to the renormalized trajectory and then along it as shown in figure 1.5.

1.2.4 Conformal Theories

In a conformal system with massless fermions, the RG flow from points on the weak coupling side of the IRFP will also flow towards the renormalized trajectory in irrelevant directions. However unlike the QCD case the flow along the renormalized trajectory will terminate at the IRFP. At the IRFP β also becomes an irrelevant operator. Had we started from the strong coupling side of the IRFP we would observe something completely new. The flow would move towards the renormalized trajectory in the irrelevant directions but it would flow into the IRFP. The flow into the IRFP from

the strong coupling is 'backwards' from the flow in a chiral broken theory. The behavior of a conformal theory is shown in figure 1.6.

1.3 8 and 12 Flavor Results

In this section I employ the two lattice matching technique described earlier in this chapter to study SU(3) gauge theories with 8 and 12 chiral fermions in the fundamental representation. We proceed by repeatedly applying an nHYP RG blocking transformations with scale factor $s = 2$. The lattices used in this study have volumes $24^3 \times 48$, $12^3 \times 24$ and $6^3 \times 12$. On the largest $24^3 \times 48$ lattices that we use in this current study, we work with fermion masses $m = 0.0025$ to stay near the $m = 0$ critical surface. Under RG blocking with scale factor s, the fermion mass changes as $s^{1+\gamma_m}$ where γ_m is the mass anomalous dimension. Therefore we use $m = 0.01$ on $12^3 \times 24$ and $m = 0.02$ on $6^3 \times 12$ lattices. We have explicitly checked that these masses are small enough to introduce only negligible finite-mass effects, by generating lattices with $m = 0$ for some points and obtaining indistinguishable results.

Under RG blocking on the $m = 0$ critical surface, the system flows toward the renormalized trajectory in irrelevant directions, and along it in the relevant direction. By blocking the larger lattices (with β_F) n_b times and the smaller lattices (with β'_F) only $n_b - 1$ times, we obtain blocked systems with the same lattice volume. If these blocked systems have both flowed to the same point on the renormalized trajectory, then we can conclude that $\xi(\beta_F) = 2\xi(\beta'_F)$ on the unblocked systems, as desired.

We determine whether the blocked systems have flowed to the same point on the renormalized trajectory by matching several short-range gauge observables: the plaquette, all three six-link loops, and two planar eight-link loops. For a given β_F, each observable may predict a different $\Delta\beta_F \equiv \beta_F - \beta'_F$. The spread in these results is a systematic error that dominates our uncertainties. In principal more observables can be added, our choices are limited by the final volume of the blocked lattice.

In an IR-conformal system, the gauge coupling that is relevant at the perturbative gaussian

FP becomes irrelevant at the IRFP. The renormalized trajectory connects these two fixed points. When RG flows approach this renormalized trajectory, the two-lattice matching can be performed and interpreted the same way as in confining systems. In this region the gauge coupling flows to stronger couplings, $\Delta\beta_F > 0$ corresponding to a negative RG β function. The situation is less clear at stronger couplings where we might naïvely expect backward flow. If there is no ultraviolet FP in this region to drive the RG flow along a renormalized trajectory, the two-lattice matching might become meaningless. This issue affects every method that attempts to determine the flow of the gauge coupling in IR-conformal systems at strong coupling. In all published studies that report an IRFP, backward flow has only been observed in a very limited range of couplings in the immediate vicinity of the IRFP (cf. Ref. [56]).

Since we can block our lattices only a few times, we must optimize the two-lattice matching by requiring that consecutive RG blocking steps yield the same $\Delta\beta_F$. We identify the optimized $\Delta\beta_F$ with the bare step-scaling function s_b. The traditional technique reported in this chapter optimizes the RG blocking transformation (renormalization scheme). The new method we propose in Section **??** instead applies the Wilson flow to the lattice system prior to RG blocking, and optimizes the flow time t_f.

As in Refs. [66, 65], we use RG blocking transformations that include two sequential HYP smearings with parameters $(\alpha, 0.2, 0.2)$, and optimize α as shown in the left panel of Fig. 1.7. Qualitatively, this optimization finds the renormalization scheme for which the renormalized trajectory passes as close as possible to the lattice system with coupling β_F. Without optimization, residual flows in irrelevant directions can distort the results: this is the reason $\Delta\beta_F$ changes with α in Fig. 1.7, and also explains why increasing the number of blocking steps reduces this α-dependence.

We note that finite-volume effects are minimized by carrying out the optimization on blocked lattices of the same volume, which was reported by Ref. [66]. That is, we should compare $\Delta\beta_F$ from matching $12^3\times24$ blocked to $3^3\times6$ vs. $6^3\times12$ blocked to $3^3\times6$ with that from matching $24^3\times48$ blocked to $3^3\times6$ vs. $12^3\times24$ blocked to $3^3\times6$. As in Refs. [66, 65], we do not explore weak enough couplings to recover the two-loop perturbative predictions $s_b \approx 0.3$ for $N_f = 12$.

1.3.1 8 Flavors

In our study of SU(3) gauge theories with 8 flavors we calculated the step scaling function at four couplings corresponding to $\beta_F = 5.4, 5.6, 6, 7$. We were unable to perform matching at stronger coupling due to the appearance of the $\not{\mathcal{S}}$ phase at $\beta_f = 4.6$. At weaker couplings our results for the step scaling function are lower than those predicted by two loop perturbation theory. Perturbation theory predicts a value of $s_b \approx 0.6$. This implies that our simulations are at couplings too strong to perform comparison to perturbation theory. Figure 1.8 displays our final results. The error bars are indicative of the spread the step scaling function predicted by different observables.

It is clear that the step scaling function is far removed from zero. This indicates that the 8 flavor theory does not have an infrared fixed point. While the calculated step scaling function is not in explicit agreement with perturbative value it is somewhat close. The fact our value for the step scaling function is below the perturbative value indicates that we are likely in strong enough coupling that perturbation theory is not reliable. Furthermore interpolating between the our measured s_b and the perturbative value does not require a fixed point to develop. This picture is consistent with 8 flavors being chirally broken and confining over the range of couplings simulated.

1.3.2 12 Flavors

Our investigation of SU(3) gauge theory with 12 flavors reveals behavior very different from the 8 flavor results. We calculated the step scaling function at $\beta_F = 5, 6, 7, 8, 9, 10$. As with the 8 flavor case we were unable to perform matching at stronger couplings because of the $\not{\mathcal{S}}$ phase at $\beta = 2.7$. At the weakest couplings studied, we find that our results for the step scaling function are smaller than those predicted by the two loop perturbative calculation which predicts $s_b \approx 0.3$. As with the 8 flavor results, this implies that we are at strong enough coupling that perturbation theory is unreliable.

The results shown in 1.9 show that the step scaling function for $\beta_F = 8, 9, 10$ is positive while the step scaling function at $\beta_F = 5, 6, 7$ is negative or close to zero. This is consistent

with backwards flow at strong couping and an infrared fixed point at $\beta_F < 8$. Unfortunately we are unable to cleanly identify where the fixed point is. I discuss this point in the next section. Independent of the location of the fixed point, our results are not consistent with a chirally broken theory.

1.3.3 The Case of the Wandering Fixed Point

Recall that our optimization of the RG blocking transformation means that we use a different renormalization scheme for each coupling β_F, so these bare step scaling functions are composites of several different discrete β functions. In an IR conformal system, each renormalization scheme has a fixed point because the existence of the fixed point is scheme independent. The location of the fixed point however is a scheme dependant property. Figure 1.10 demonstrates how this can happen and complicate locating the IRFP. Therefore it is reasonable to expect the IRFP to be located at a different point in coupling space for each β_F that we calculate s_b for. For example, with $N_f = 12$ at $5 \leq \beta_F \leq 6$, our optimization selects renormalization schemes with the fixed point near β_F, so that s_b is roughly consistent with zero over an extended range.

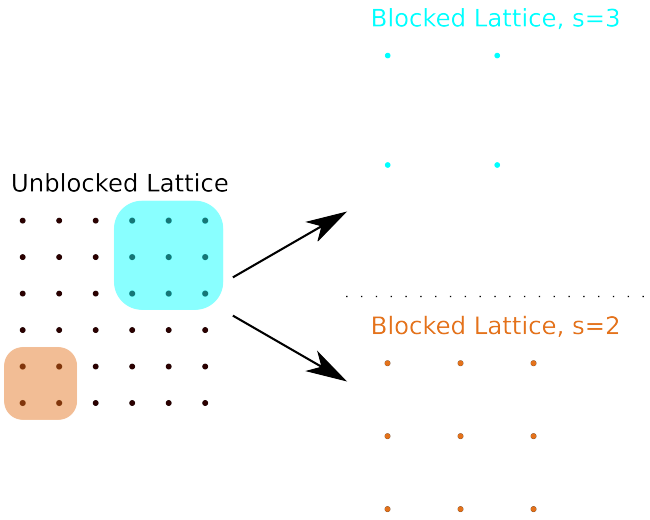

Figure 1.1: The original 6x6 lattice on the left possesses a discrete scaling symmetry of $s = 2$ and $s = 3$. The shaded orange square is a $s = 2$ block variable. The resulting orange 3×3 blocked lattice in the bottom right formed by replacing each block variable with a single site in the upper left corner of the block. The cyan shaded region shows a $b = 3$ block variable. Performing a block transformation that replaces each block with a point in the upper left of the block produces the 2×2 blocked lattice shown in the upper right.

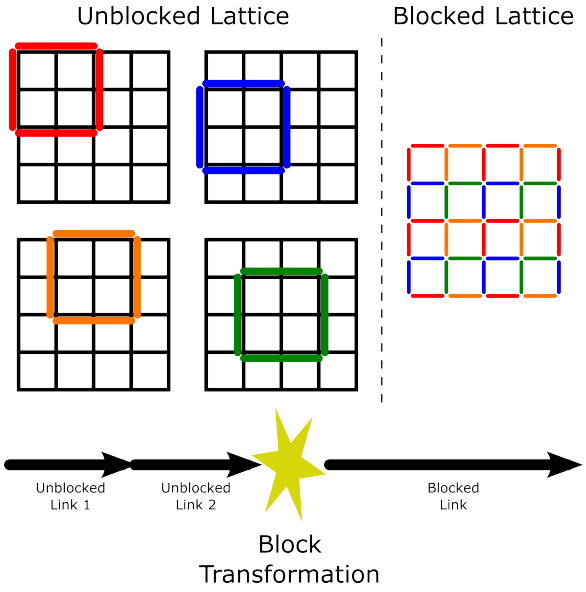

Figure 1.2: This figure shows how links are blocked on the lattice. Two adjacent links in the same direction are block transformed to form one link of twice the lattice spacing. We perform all possible block transformation shown on the left as the red, blue, green, and orange block tilings of the unblocked lattice. We then store the links of the blocked lattice as shown on the right hand side of the figure.

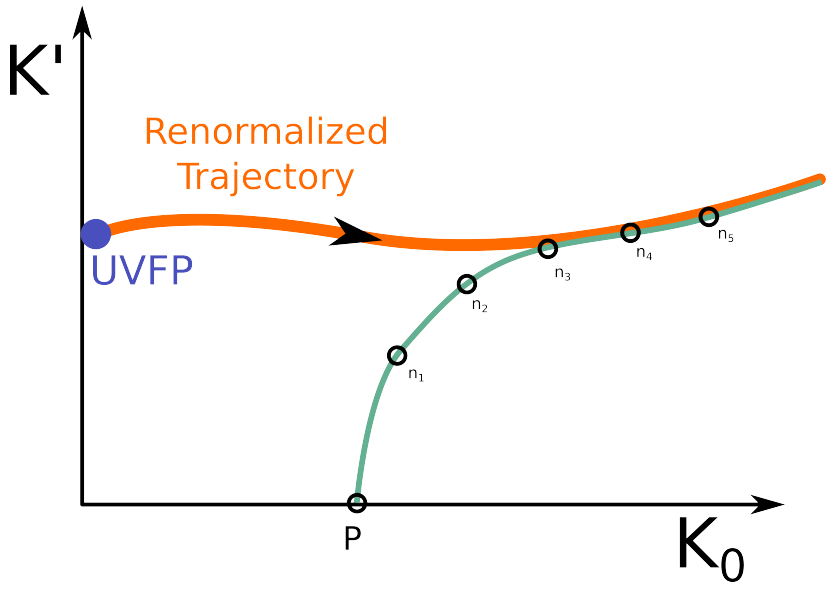

Figure 1.3: Here I show coupling space for a system with one relevant direction K_0. All irrelevant directions are collected in K'. We simulate at a point P in parameter. As we block the system it the effective couplings will change. In the diagram here the couplings reach the renormalized trajectory after 3 blocking steps. Further blocking steps move the couplnigs along the renormalized trajectory.

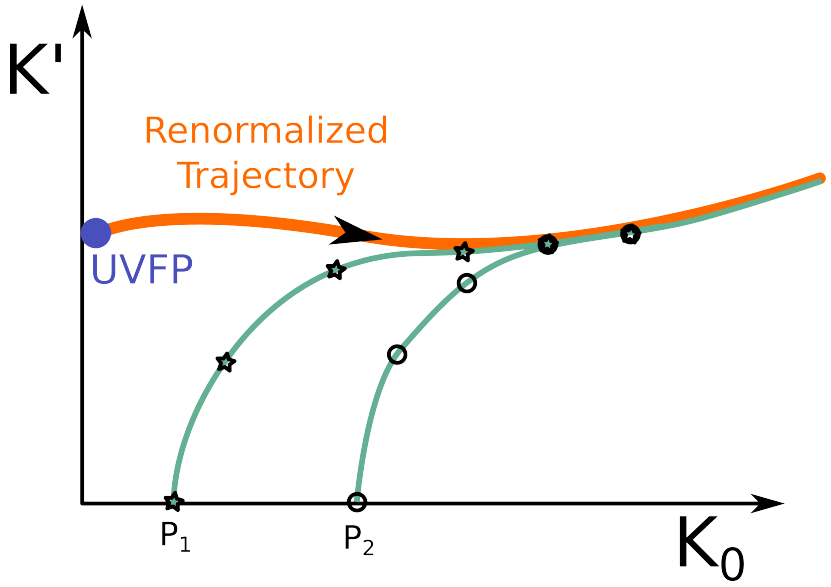

Figure 1.4: For matching we pick two points in coupling space P_1 and P_2. After 3 blocking steps, shown as circles the effective action of P_2 has reached the renormalized trajectory. P_1 requires 4 blocking steps shown as stars but reahes the same point on the renormalized trajectory. Because P_2 took one less blockign step its correlation length ξ is a factor of s smaller than the correlation length of the first ensemble that started at P_1. By choosing pairs of points in coupling space that block to the same point on the renormalized trajectory in coupling space, we can construct a discrete step scaling function.

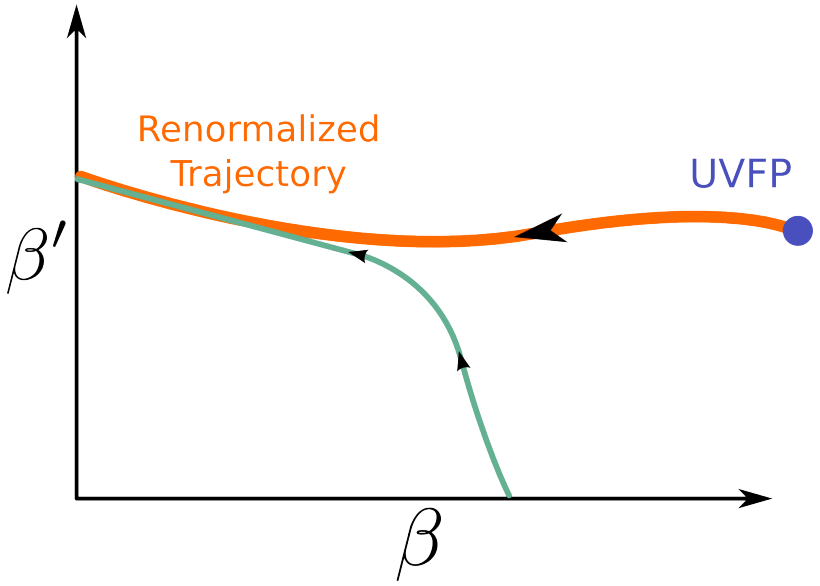

Figure 1.5: The RG flow of a confining theory on the $m = 0$ critical surface. β is the relevant gauge coupling, β' are irrelevant couplings.

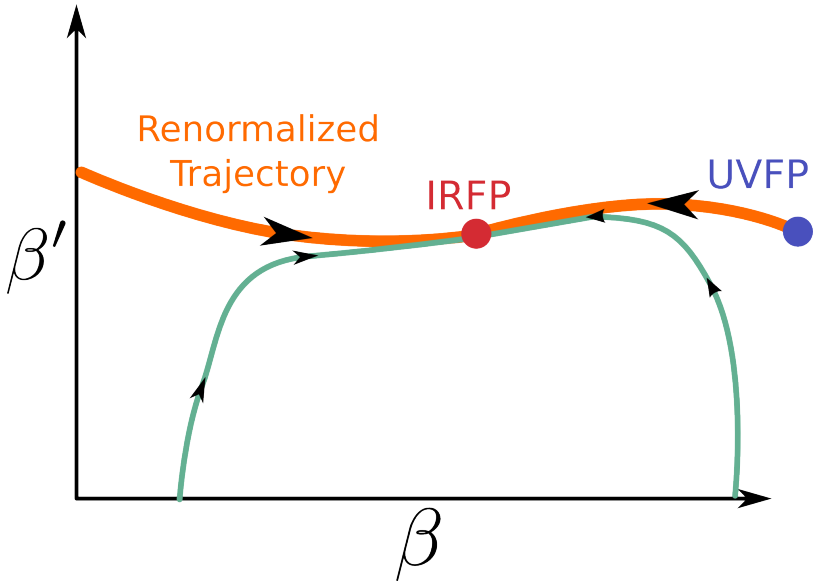

Figure 1.6: The RG flow of a conformal theory on the $m = 0$ critical surface. β is the relevant gauge coupling, β' are irrelevant couplings.

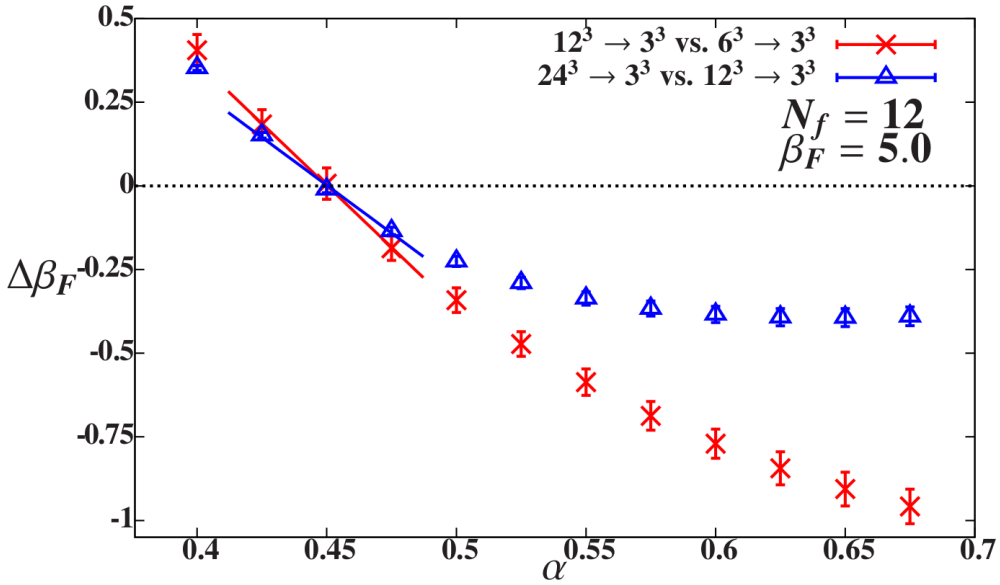

Figure 1.7: Optimization of the HYP-smearing parameter α in the RG blocking transformation, for $\beta_F = 5.0$. The uncertainties on the data points are dominated by averaging over the different observables as described in the text.

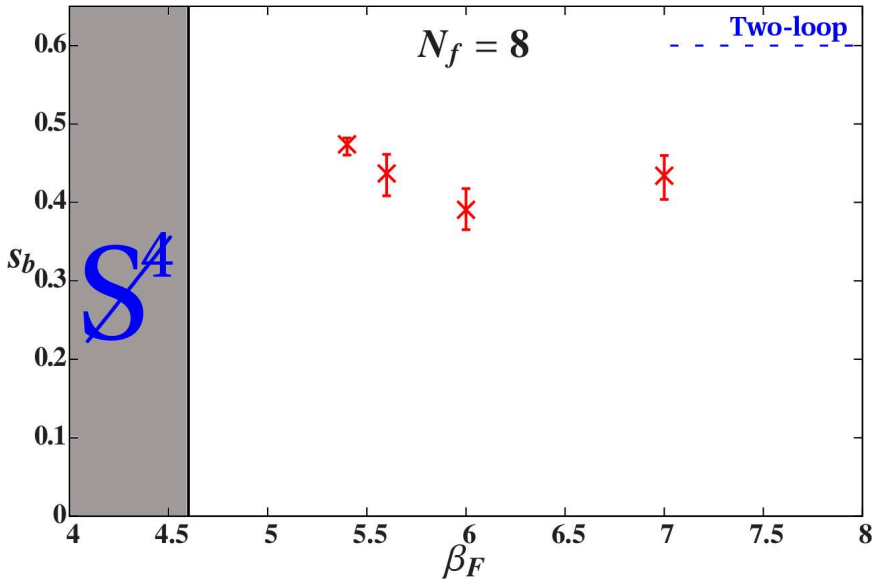

Figure 1.8: Results for the bare step-scaling function s_b from traditional MCRG two-lattice matching with $24^3 \times 48$, $12^3 \times 24$ and $6^3 \times 12$ lattice volumes for $N_f = 8$. The blue dashed lines are perturbative predictions for asymptotically weak coupling.

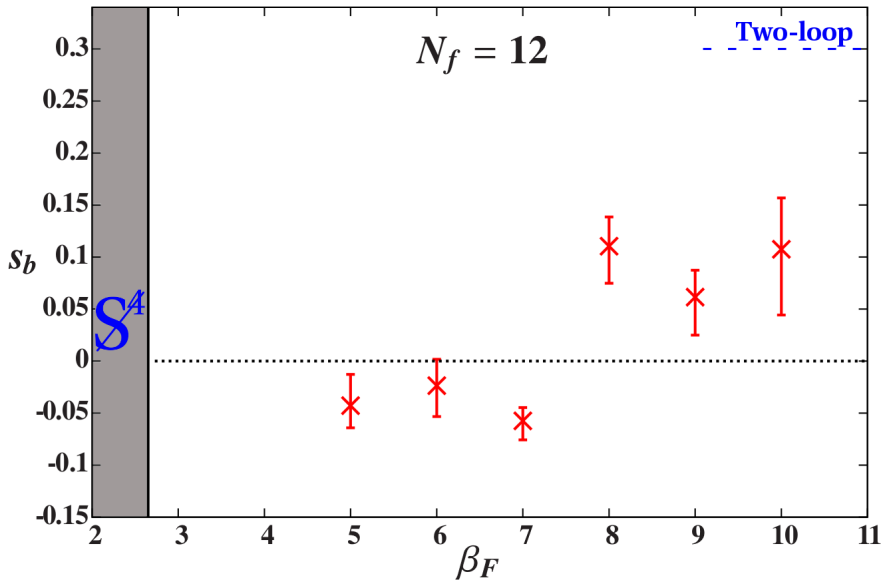

Figure 1.9: Results for the bare step-scaling function s_b from traditional MCRG two-lattice matching with $24^3 \times 48$, $12^3 \times 24$ and $6^3 \times 12$ lattice volumes for $N_f = 12$. The blue dashed lines are perturbative predictions for asymptotically weak coupling.

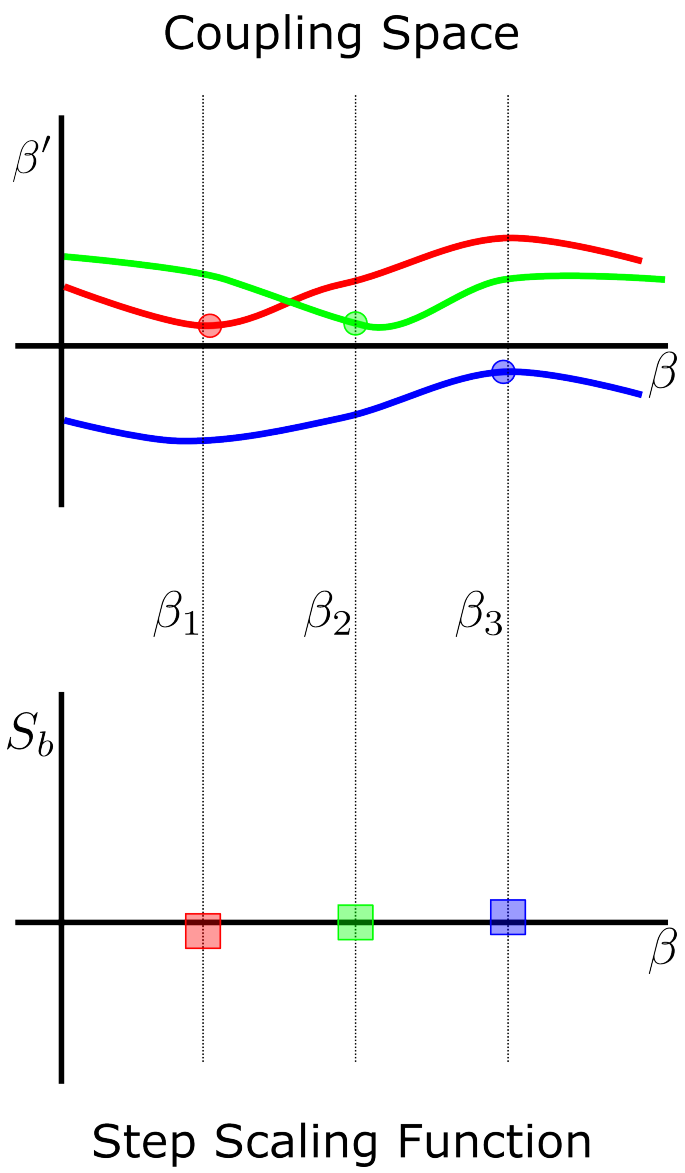

Figure 1.10: An illustration of how optimizing the block transformation can result in difficulties locating an IRFP, β is the relevant gauge coupling and β' are irrelevant couplings. The upper figure shows the renormalized trajectory in red, green, and blue found by optimizing the RG transformation at $\beta_1, \beta_2,$ andβ_3 respectively. The location of the IRFP changes in each renormalized trajectory, in this picture the IRFP is moved to the coupling we perform MCRG at. The resulting s_b is consistent with zero across a wide range of couplings.

Bibliography

[1]

[2] David Adams. Fourth root prescription for dynamical staggered fermions. Phys. Rev. D, 72:114512, Dec 2005.

[3] Yasumichi Aoki, Tatsumi Aoyama, Masafumi Kurachi, Toshihide Maskawa, Kohtaroh Miura, Kei-ichi Nagai, Hiroshi Ohki, Enrico Rinaldi, Akihiro Shibata, Koichi Yamawaki, and Takeshi Yamazaki. Light composite scalar in eight-flavor QCD on the lattice. 2014.

[4] Yasumichi Aoki, Tatsumi Aoyama, Masafumi Kurachi, Toshihide Maskawa, Kei-ichi Nagai, Hiroshi Ohki, Enrico Rinaldi, Akihiro Shibata, Koichi Yamawaki, and Takeshi Yamazaki. Light composite scalar in twelve-flavor QCD on the lattice. Phys. Rev. Lett., 111:162001, 2013.

[5] Yasumichi Aoki, Tatsumi Aoyama, Masafumi Kurachi, Toshihide Maskawa, Kei-ichi Nagai, Hiroshi Ohki, Enrico Rinaldi, Akihiro Shibata, Koichi Yamawaki, and Takeshi Yamazaki. The scalar spectrum of many-flavour QCD. 2013.

[6] Yasumichi Aoki, Tatsumi Aoyama, Masafumi Kurachi, Toshihide Maskawa, Kei-ichi Nagai, Hiroshi Ohki, Akihiro Shibata, Koichi Yamawaki, and Takeshi Yamazaki. Lattice study of conformality in twelve-flavor QCD. Phys. Rev., D86:054506, 2012.

[7] T. Appelquist, G. T. Fleming, M. F. Lin, E. T. Neil, and D. Schaich. Lattice Simulations and Infrared Conformality. Phys. Rev., D84:054501, 2011.

[8] Thomas Appelquist, Richard Brower, Simon Catterall, George Fleming, Joel Giedt, Anna Hasenfratz, Julius Kuti, Ethan Neil, and David Schaich. Lattice Gauge Theories at the Energy Frontier. 2013.

[9] Thomas Appelquist, George T. Fleming, and Ethan T. Neil. Lattice study of the conformal window in QCD-like theories. Phys. Rev. Lett., 100:171607, 2008.

[10] Thomas Appelquist, George T. Fleming, and Ethan T. Neil. Lattice Study of Conformal Behavior in SU(3) Yang-Mills Theories. Phys. Rev., D79:076010, 2009.

[11] Thomas Appelquist and Ethan T. Neil. Lattice gauge theory beyond the standard model. pages 699–729, 2009.

[12] Janos Balog, Ferenc Niedermayer, and Peter Weisz. Logarithmic corrections to O(a**2) lattice artifacts. Phys. Lett., B676:188–192, 2009.

[13] Janos Balog, Ferenc Niedermayer, and Peter Weisz. The Puzzle of apparent linear lattice artifacts in the 2d non-linear sigma-model and Symanzik's solution. Nucl. Phys., B824:563–615, 2010.

[14] Tom Banks and A. Zaks. On the Phase Structure of Vector-Like Gauge Theories with Massless Fermions. Nucl. Phys., B196:189, 1982.

[15] Claude Bernard, Maarten Golterman, Yigal Shamir, and Stephen R. Sharpe. Comment on: chiral anomalies and rooted staggered fermions [phys. lett. b 649 (2007) 230]. Physics Letters B, 649(23):235 – 240, 2007.

[16] Gyan Bhanot. Su(3) lattice gauge theory in 4 dimensions with a modified wilson action. Physics Letters B, 108(45):337 – 340, 1982.

[17] Gyan Bhanot and Michael Creutz. Variant actions and phase structure in lattice gauge theory. Phys. Rev. D, 24:3212–3217, Dec 1981.

[18] J. Binney, N.J. Dowrick, A.J. Fisher, and M.E.J. Newman. The Theory of Critical Phenomena: An Introduction to the Renormalization Group. Oxford University Press, Oxford, 1992.

[19] T. Blum, C. DeTar, Urs M. Heller, Leo Krkkinen, K. Rummukainen, and D. Toussaint. Thermal phase transition in mixed action {SU} (3) lattice gauge theory and wilson fermion thermodynamics. Nuclear Physics B, 442(12):301 – 316, 1995.

[20] A. Bode. Two loop expansion of the schrdinger functional coupling sf in {SU} (3) lattice gauge theory. Nuclear Physics B - Proceedings Supplements, 63(13):796 – 798, 1998. Proceedings of the {XVth} International Symposium on Lattice Field Theory.

[21] Szabolcs Borsanyi, Stephan Durr, Zoltan Fodor, Christian Hoelbling, Sandor D. Katz, S. Krieg, T. Kurth, L. Lellouch, T. Lippert, C. McNeile, and K. K. Szabo. High-precision scale setting in lattice QCD. JHEP, 1209:010, 2012.

[22] William E. Caswell. Asymptotic Behavior of Nonabelian Gauge Theories to Two Loop Order. Phys. Rev. Lett., 33:244, 1974.

[23] Simon Catterall and Francesco Sannino. Minimal walking on the lattice. Phys.Rev., D76:034504, 2007.

[24] Anqi Cheng, Anna Hasenfratz, Yuzhi Liu, Gregory Petropoulos, and David Schaich. Finite size scaling of conformal theories in the presence of a near-marginal operator. 2013.

[25] Anqi Cheng, Anna Hasenfratz, Yuzhi Liu, Gregory Petropoulos, and David Schaich. Step scaling studies using the gradient flow running coupling. 2014, in preparation.

[26] Anqi Cheng, Anna Hasenfratz, Gregory Petropoulos, and David Schaich. Determining the mass anomalous dimension through the eigenmodes of Dirac operator. PoS, LATTICE 2013:088, 2013.

[27] Anqi Cheng, Anna Hasenfratz, Gregory Petropoulos, and David Schaich. Scale-dependent mass anomalous dimension from Dirac eigenmodes. JHEP, 1307:061, 2013.

[28] Anqi Cheng, Anna Hasenfratz, and David Schaich. Novel phase in SU(3) lattice gauge theory with 12 light fermions. Phys. Rev., D85:094509, 2012.

[29] Christian B. Lang Christof Gattringer. Quantum Chromodynamics on the Lattice. Springer, 2010.

[30] Michael Creutz. Chiral anomalies and rooted staggered fermions. Physics Letters B, 649(23):230 – 234, 2007.

[31] Michael Creutz. Reply to: comment on: chiral anomalies and rooted staggered fermions [phys. lett. b 649 (2007) 230] [phys. lett. b 649 (2007) 235]. Physics Letters B, 649(23):241 – 242, 2007.

[32] Thomas DeGrand. Lattice studies of QCD-like theories with many fermionic degrees of freedom. 2010.

[33] Thomas DeGrand. Finite-size scaling tests for spectra in SU(3) lattice gauge theory coupled to 12 fundamental flavor fermions. Phys. Rev., D84:116901, 2011.

[34] Thomas DeGrand and Anna Hasenfratz. Remarks on lattice gauge theories with infrared-attractive fixed points. Phys.Rev., D80:034506, 2009.

[35] Thomas DeGrand, Yigal Shamir, and Benjamin Svetitsky. Gauge theories with fermions in the two-index symmetric representation. PoS, LATTICE2011:060, 2011.

[36] Thomas DeGrand, Yigal Shamir, and Benjamin Svetitsky. Infrared fixed point in SU(2) gauge theory with adjoint fermions. Phys.Rev., D83:074507, 2011.

[37] Luigi Del Debbio, Biagio Lucini, Agostino Patella, Claudio Pica, and Antonio Rago. Mesonic spectroscopy of Minimal Walking Technicolor. Phys.Rev., D82:014509, 2010.

[38] T. DeGrand & C DeTar. Lattice Methods for Quantum Chromodynamics. World Scientific, 2006.

[39] A. Deuzeman, M. P. Lombardo, and E. Pallante. Evidence for a conformal phase in SU(N) gauge theories. Phys. Rev., D82:074503, 2010.

[40] Albert Deuzeman, Maria Paola Lombardo, Tiago Nunes da Silva, and Elisabetta Pallante. The bulk transition of QCD with twelve flavors and the role of improvement. 2012.

[41] Savas Dimopoulos and Leonard Susskind. Mass Without Scalars. Nucl.Phys., B155:237–252, 1979.

[42] Michael Dine. Tasi lectures on the strong cp problem.

[43] Estia Eichten and Kenneth D. Lane. Dynamical Breaking of Weak Interaction Symmetries. Phys.Lett., B90:125–130, 1980.

[44] F. Englert and R. Brout. Broken Symmetry and the Mass of Gauge Vector Mesons. Phys.Rev.Lett., 13:321–323, 1964.

[45] Zoltan Fodor, Kieran Holland, Julius Kuti, Daniel Nogradi, and Chris Schroeder. Nearly conformal gauge theories on the lattice. Int.J.Mod.Phys., A25:5162–5174, 2010.

[46] Zoltan Fodor, Kieran Holland, Julius Kuti, Daniel Nogradi, and Chris Schroeder. Twelve massless flavors and three colors below the conformal window. Phys. Lett., B703:348–358, 2011.

[47] Zoltan Fodor, Kieran Holland, Julius Kuti, Daniel Nogradi, Chris Schroeder, and Chik Him Wong. Can the nearly conformal sextet gauge model hide the Higgs impostor? Phys. Lett., B718:657–666, 2012.

[48] Zoltan Fodor, Kieran Holland, Julius Kuti, Daniel Nogradi, Chris Schroeder, and Chik Him Wong. Confining force and running coupling with twelve fundamental and two sextet fermions. PoS, Lattice 2012:025, 2012.

[49] Zoltan Fodor, Kieran Holland, Julius Kuti, Daniel Nogradi, Chris Schroeder, and Chik Him Wong. Conformal finite size scaling of twelve fermion flavors. PoS, Lattice 2012:279, 2012.

[50] Zoltan Fodor, Kieran Holland, Julius Kuti, Daniel Nogradi, and Chik Him Wong. The gradient flow running coupling scheme. PoS, Lattice 2012:050, 2012.

[51] Zoltan Fodor, Kieran Holland, Julius Kuti, Daniel Nogradi, and Chik Him Wong. The Yang-Mills gradient flow in finite volume. JHEP, 1211:007, 2012.

[52] Zoltan Fodor, Kieran Holland, Julius Kuti, Daniel Nogradi, and Chik Him Wong. Can a light Higgs impostor hide in composite gauge models? PoS, LATTICE 2013:062, 2014.

[53] Patrick Fritzsch and Alberto Ramos. The gradient flow coupling in the Schrdinger Functional. JHEP, 1310:008, 2013.

[54] J. Gasser and H. Leutwyler. Chiral perturbation theory to one loop. Ann. Phys., 158:142, 1984.

[55] Howard Georgi and David B. Kaplan. Composite Higgs and Custodial SU(2). Phys.Lett., B145:216, 1984.

[56] Joel Giedt. Confining force and running coupling with twelve fundamental and two sextet fermions. PoS, Lattice 2012:006, 2012.

[57] Joel Giedt. Lattice gauge theory and physics beyond the standard model. PoS, Lattice 2012:006, 2012.

[58] Sheldon L. Glashow. Partial-symmetries of weak interactions. Nuclear Physics, 22(4):579 – 588, 1961.

[59] Maarten Golterman. Applications of chiral perturbation theory to lattice QCD. pages 423–515, 2009.

[60] David Gross and Frank Wilczek. Ultraviolet behavior of non-abelian gauge theories. Phys. Rev. Lett., 30:1343–1346, Jun 1973.

[61] G.S. Guralnik, C.R. Hagen, and T.W.B. Kibble. Global Conservation Laws and Massless Particles. Phys.Rev.Lett., 13:585–587, 1964.

[62] A. Hasenfratz, R. Hoffmann, and F. Knechtli. The Static potential with hypercubic blocking. Nucl.Phys.Proc.Suppl., 106:418–420, 2002.

[63] Anna Hasenfratz. Investigating the critical properties of beyond-qcd theories using monte carlo renormalization group matching. Phys. Rev. D, 80:034505, Aug 2009.

[64] Anna Hasenfratz. Conformal or Walking? Monte Carlo renormalization group studies of SU(3) gauge models with fundamental fermions. Phys. Rev., D82:014506, 2010.

[65] Anna Hasenfratz. MCRG study of 12 fundamental flavors with mixed fundamental-adjoint gauge action. PoS, Lattice 2011:065, 2011.

[66] Anna Hasenfratz. Infrared fixed point of the 12-fermion SU(3) gauge model based on 2-lattice MCRG matching. Phys. Rev. Lett., 108:061601, 2012.

[67] Anna Hasenfratz, Anqi Cheng, Gregory Petropoulos, and David Schaich. Mass anomalous dimension from Dirac eigenmode scaling in conformal and confining systems. PoS, Lattice 2012:034, 2012.

[68] Anna Hasenfratz, Anqi Cheng, Gregory Petropoulos, and David Schaich. Finite size scaling and the effect of the gauge coupling in 12 flavor systems. PoS, LATTICE 2013:075, 2013.

[69] Anna Hasenfratz, Anqi Cheng, Gregory Petropoulos, and David Schaich. Reaching the chiral limit in many flavor systems. 2013.

[70] Anna Hasenfratz, Roland Hoffmann, and Stefan Schaefer. Hypercubic smeared links for dynamical fermions. JHEP, 0705:029, 2007.

[71] Anna Hasenfratz and Francesco Knechtli. Flavor symmetry and the static potential with hypercubic blocking. Phys. Rev., D64:034504, 2001.

[72] Anna Hasenfratz, David Schaich, and Aarti Veernala. Nonperturbative beta function of eight-flavor SU(3) gauge theory. 2014.

[73] Peter W. Higgs. Broken symmetries and the masses of gauge bosons. Phys. Rev. Lett., 13(16):508–509, October 1964.

[74] P.W. Higgs. Broken symmetries, massless particles and gauge fields. Physics Letters, 12(2):132 – 133, 1964.

[75] Christopher T. Hill and Elizabeth H. Simmons. Strong dynamics and electroweak symmetry breaking. Physics Reports, 381(46):235 – 402, 2003.

[76] Etsuko Itou. Properties of the twisted Polyakov loop coupling and the infrared fixed point in the SU(3) gauge theories. PTEP, 2013:083B01, 2013.

[77] Y. Iwasaki, K. Kanaya, S. Kaya, S. Sakai, and T. Yoshie. Phase structure of lattice QCD for general number of flavors. Phys.Rev., D69:014507, 2004.

[78] Xiao-Yong Jin and Robert D. Mawhinney. Lattice QCD with Eight Degenerate Quark Flavors. PoS, LATTICE2008:059, 2008.

[79] Xiao-Yong Jin and Robert D. Mawhinney. Lattice QCD with 8 and 12 degenerate quark flavors. PoS, LAT2009:049, 2009.

[80] Xiao-Yong Jin and Robert D. Mawhinney. Lattice QCD with 12 Degenerate Quark Flavors. PoS, Lattice 2011:066, 2012.

[81] David B. Kaplan, Howard Georgi, and Savas Dimopoulos. Composite Higgs Scalars. Phys.Lett., B136:187, 1984.

[82] D.B. Kaplan. Chiral symmetry and lattice fermions.

[83] John Kogut and Leonard Susskind. Hamiltonian formulation of wilson's lattice gauge theories. Phys. Rev. D, 11:395–408, Jan 1975.

[84] Andreas S. Kronfeld. Lattice gauge theory with staggered fermions: How, where, and why (not). PoS, LAT2007:016, 2007.

[85] Kenneth Lane. Two lectures on technicolor.

[86] C.-J. David Lin, Kenji Ogawa, Hiroshi Ohki, and Eigo Shintani. Lattice study of infrared behaviour in SU(3) gauge theory with twelve massless flavours. JHEP, 1208:096, 2012.

[87] Martin Luscher. Properties and uses of the Wilson flow in lattice QCD. JHEP, 1008:071, 2010.

[88] Martin Luscher. Trivializing maps, the Wilson flow and the HMC algorithm. Commun. Math. Phys., 293:899–919, 2010.

[89] M. Lscher and P. Weisz. Computation of the action for on-shell improved lattice gauge theories at weak coupling. Physics Letters B, 158(3):250 – 254, 1985.

[90] Adam Martin. Technicolor signals at the lhc.

[91] Shinya Matsuzaki and Koichi Yamawaki. Holographic techni-dilaton at 125 GeV. Phys. Rev., D86:115004, 2012.

[92] R. Narayanan and H. Neuberger. Infinite N phase transitions in continuum Wilson loop operators. JHEP, 0603:064, 2006.

[93] Ethan T. Neil. Exploring Models for New Physics on the Lattice. PoS, Lattice 2011:009, 2011.

[94] H.B. Nielsen and M. Ninomiya. Absence of neutrinos on a lattice: (i). proof by homotopy theory. Nuclear Physics B, 185(1):20 – 40, 1981.

[95] H.B. Nielsen and M. Ninomiya. Absence of neutrinos on a lattice: (ii). intuitive topological proof. Nuclear Physics B, 193(1):173 – 194, 1981.

[96] H.B. Nielsen and M. Ninomiya. A no-go theorem for regularizing chiral fermions. Physics Letters B, 105(23):219 – 223, 1981.

[97] Paula Perez-Rubio and Stefan Sint. Non-perturbative running of the coupling from four flavour lattice QCD with staggered quarks. PoS, Lattice 2010:236, 2010.

[98] Michael E. Peskin and Dan V. Schroeder. An Introduction To Quantum Field Theory (Frontiers in Physics). Westview Press, 1995.

[99] Gregory Petropoulos, Anqi Cheng, Anna Hasenfratz, and David Schaich. PoS, Lattice 2012:051, 2012.

[100] Gregory Petropoulos, Anqi Cheng, Anna Hasenfratz, and David Schaich. Improved Lattice Renormalization Group Techniques. PoS, LATTICE 2013:079, 2013.

[101] H. David Politzer. Reliable Perturbative Results for Strong Interactions? Phys.Rev.Lett., 30:1346–1349, 1973.

[102] C. Quigg. Spontaneous symmetry breaking as a basis of particle mass. Rept. Prog. Physics, pages 1019–1054, 2007.

[103] C. Quigg. Unanswered questions in the electroweak theory. Annual Review of Nuclear and Particle Science, pages 505–555, 2009.

[104] Thomas A. Ryttov and Robert Shrock. An Analysis of Scheme Transformations in the Vicinity of an Infrared Fixed Point. Phys.Rev., D86:085005, 2012.

[105] Abdus Salam and John Clive Ward. Electromagnetic and weak interactions. Phys. Lett., 13:168–171, 1964.

[106] Francesco Sannino. Conformal Dynamics for TeV Physics and Cosmology. Acta Phys.Polon., B40:3533–3743, 2009.

[107] David Schaich, Anqi Cheng, Anna Hasenfratz, and Gregory Petropoulos. Bulk and finite-temperature transitions in SU(3) gauge theories with many light fermions. PoS, Lattice 2012:028, 2012.

[108] Robert Shrock. Some recent results on models of dynamical electroweak symmetry breaking. pages 227–241, 2007.

[109] Stefan Sint. On the schrdinger functional in {QCD}. Nuclear Physics B, 421(1):135 – 156, 1994.

[110] Jan Smit. Introduction to Quantum Fields on a Lattice. Cambridge University Press, 2002.

[111] Rainer Sommer. Scale setting in lattice QCD. PoS, LATTICE 2013:015, 2014.

[112] Leonard Susskind. Dynamics of Spontaneous Symmetry Breaking in the Weinberg-Salam Theory. Phys.Rev., D20:2619–2625, 1979.

[113] R.H. Swendsen. Phys. Rev. Lett., 42:859, 1979.

[114] K. Symanzik. Continuum limit and improved action in lattice theories : (ii). o(n) non-linear sigma model in perturbation theory. Nuclear Physics B, 226(1):205 – 227, 1983.

[115] Fatih Tekin, Rainer Sommer, and Ulli Wolff. The Running coupling of QCD with four flavors. Nucl. Phys., B840:114–128, 2010.

[116] Steven Weinberg. A Model of Leptons. Phys.Rev.Lett., 19:1264–1266, 1967.

[117] Steven Weinberg. Implications of Dynamical Symmetry Breaking. Phys.Rev., D13:974–996, 1976.

[118] Steven Weinberg. Implications of Dynamical Symmetry Breaking: An Addendum. Phys.Rev., D19:1277–1280, 1979.

[119] P. Weisz. Continuum limit improved lattice action for pure yang-mills theory (i). Nuclear Physics B, 212(1):1 – 17, 1983.

[120] Kenneth Wilson. Confinement of quarks. Phys. Rev. D, 10:2445–2459, Oct 1974.